Numerical study on the energy extraction performance of coupled tandem flapping hydrofoils

Qu Hengliang, Xu Chuanli, Zhang Xiaoxia, Qu Na, Liu Zhen

Abstract—**Tidal current energy is a promising renewable energy source for the future electricity supply. The flapping foil is regarded as a useful tool to extract the tidal current energy in shallow water. A concept of coupled tandem flapping hydrofoils is proposed in the present study. And a numerical study is carried out to optimize the system of the tandem flapping hydrofoils for more energy extraction. A two-dimensional numerical model, based on ANSYS-Fluent, is established to study the power extraction performance, which is validated by corresponding experiment data. Effects of the reduced frequency, pitching amplitude and moment of inertia are investigated. The vortices and pressure distribution of hydrofoils under various conditions are analysed to reveal the fluid-structure interaction between the shedding vortex and the foils. The energy extraction mechanism and hydrodynamic performance are analysed. The positive interactions for energy harvesting are expected to be identified for further improvements. The study could provide valuable information for the design and optimization of coupled tandem flapping hydrofoils.**

Keywords—**Energy extraction, Numerical study, Coupled tandem hydrofoils**

I. Introduction

TIDAL current energy converter can be classified into three major types, horizontal-axis turbine, and vertical-axis turbine and flapping hydrofoil. Flapping hydrofoil is believed to have some advantages over rotational turbines. Low tip speed ratio which contributes to reducing negative impact on environment; Flapping hydrofoil can operate in shallow water due to the rectangular swept window [1,2]. Extensive studies on the flapping foil for energy harvesting are continued. Considering high power extraction efficiency requirement and the special structure of flapping foil, the tandem flapping hydrofoils are proposed because the same flow window can be shared by the two hydrofoils, which allows the hydrofoils to reach higher efficiencies [3]. Kinsey and Dumas [4,5] tested the concept of tandem flapping hydrofoils by the prototype experiment. The heaving motion and pitching motion can be transmitted to the electric generator through a series of link mechanisms. The results from the experiment show that the hydrodynamic power extraction efficiency can reach up to 40%. A series of numerical studies are carried out by Kinsey and Dumas [6] for optimizing the configuration of tandem flapping hydrofoils. The positive interactions between the downstream foil and wake vortices generated by the upstream foil contribute to a higher efficiency which is up to 64%. And the interactions are determined by the relative position and motion phase shift of the two foils [7]. Karbasian et al. [8] studied the power extraction performance of multiple hydrofoils in tandem formation. It is found that the overall power efficiency would increase with the number of hydrofoils increasing, and after a certain number, the overall power efficiency would be independent of hydrofoil numbers. The peak of the overall power efficiency reported in the paper is up to 95% within 15 stages of hydrofoils. Timothy and Lian [9] established the 3D numerical simulation to investigate the vortex structure and interaction between the upstream and downstream hydrofoils. The 3D simulation results showed that a weaker leading edge vortex was generated due to the 3D effect, and the interaction between upstream and downstream hydrofoils was weaker than that predicted by the 2D simulation. Xu [10] studied the energy extraction of tandem flapping hydrofoils based on velocity potential theory. The global phase shift determined by the longitudinal distance and the phase shift of the motions of the two foils has been investigated and analyzed.

Most previous studies of tandem flapping hydrofoils concentrated on the power extraction performance optimization and the interaction between the upstream and downstream foils via experiments and numerical simulations. The tandem foils of the prototype

ID: 1830 Track: Tidal device development and testing

The research comes from the project fully supported by the National Natural Science Foundation of China (Grant No.: 51779239), the Key Basic Program of Shandong Natural Science Funds (Grant No.: ZR2017ZA0202), Qingdao Livelihood S&T Project (Grant No.: 17-6-3-25-gx) and the Program of Introducing Talents of Discipline to Universities ("111" project, Grant No. B14028).

Q. Hengliang is at College of engineering, Ocean University of China, Qingdao, China, 266100 (e-mail: quhengliang@stu.ouc.edu.cn).

L. Zhen is at College of Engineering, Ocean University of China, Qingdao, China, 266100 (e-mail: liuzhen@ouc.edu.cn).

experiment [4,11] are actuated by the flow without external drive train, while the motions of foils especially the amplitudes of heaving and pitching motions are limited by the link mechanism. Meanwhile the upstream and downstream foils are connected by one rod, which means the motions of the two foils would be interacted on each other. Most numerical studies like [12-15] applied the full-activated controlling strategy to prescribe the typical sinusoidal heaving and pitching motions. Thus, the motion interactions of the two tandem foils are ignored, which is not realistic for the practical application.

In this paper, the numerical simulation based on semi-activated controlling strategy is performed to investigate the coupled tandem flapping hydrofoils, and the motions are linked. The fluid-structure interaction modelling and the numerical model based on the CFD software Fluent are described in Section 2. In Section 3, variations in flow fields, hydrodynamic torques, forces and power efficiencies are analysed. The main conclusions derived from the results are discussed in Section 4.

II. NUMERICAL MODEL

The tandem configuration of two coupled foils is shown in Fig. 1. The tandem consists of an upstream foil and a downstream foil interconnected by a rod. The rod is restricted to pitch only by the shaft. The 2D numerical model is set up based on the prototype of Kinsey. The incident velocity U is fixed at 2 m/s. The profile of foils is NACA0015, and the chord length of foils is defined as c, which is fixed at 0.24 m. The pitching axis is located at $c/3$. The instantaneous pitching angular and heaving angular are defined as $\theta(t)$ and $\alpha(t)$, respectively. The inter-foil spacing is defined as L, which is fixed at 1.296 m. In addition, the positive directions of moment and angular velocity are defined to be clockwise.

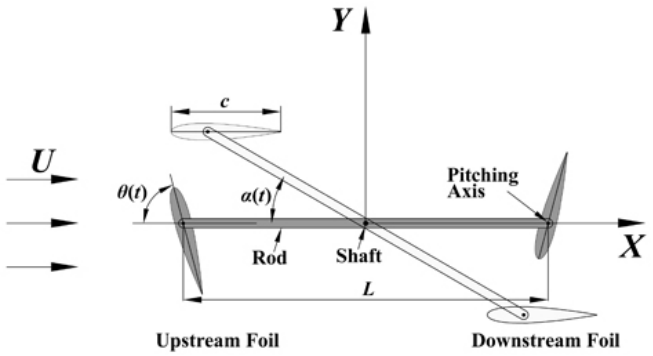

Fig. 1. Schematic of coupled tandem flapping hydrofoils.

The heaving motion and pitching motion of the foils under the restriction of the rod are determined by the Newton's second law and realized using the user-defined function (UDF) in the computation platform. The fundamental and the flow are as follows. First, the pressure distribution all over the hydrofoil can be derived after initializing the calculation. The resultant torques about the shaft and the pivot are integrated. The angular acceleration and the angular velocity at this time step can be calculated. The angular positions of the foils are updated, and the new solid boundary to the water is reformed. The renewed flow field is subsequently employed in the next-round calculation.

The governing equation of the hydrofoils pitching motion can be defined as:

$$\theta(t) = \theta_0 cos(2\pi f t) \tag{1}$$

where θ_0 is the pitching amplitude, f is the frequency. It should be noted that $\theta(t)$ of the upstream foil and downstream foil is equal in magnitude and opposite in direction.

The heaving motion is governed by the Newton's second law, and the specific equation is defined as:

$$I\frac{d\omega}{dt} + T_L = T_U + T_D \tag{2}$$

where I is the moment of inertia about the shaft. ω is the heaving angular velocity, and t is the time. T_L denotes the resistive load torque from the damper which is proportional to the heaving angular velocity. $T_L = C_d\omega$, and C_d is the damping coefficient. T_U and T_D are the hydrodynamic torque about the shaft integrated from the upstream and downstream foils, respectively.

The heaving angular velocity at the time of $t + \Delta t$ can be calculated as:

$$\omega_{t+\Delta t} = \omega_t + \frac{(T_U + T_D - T_L)|_t}{I}\Delta t \tag{3}$$

Furthermore, the instantaneous heaving angular position at the same time of $t + \Delta t$ can be calculated as:

$$\alpha_{t+\Delta t} = \alpha_t + \omega_{t+\Delta t}\Delta t \tag{4}$$

The computational domain and mesh structures are shown in Fig.2. The straight line, located at $6c$ away from the upstream foil pivot at the left side, is set as velocity inlet boundary. The straight line, located at $9c$ away from the downstream foil pivot at the right side, is set as the pressure outlet boundary. The upper and lower boundaries are both $5c$ away from the foil and set as the symmetry boundaries, respectively.

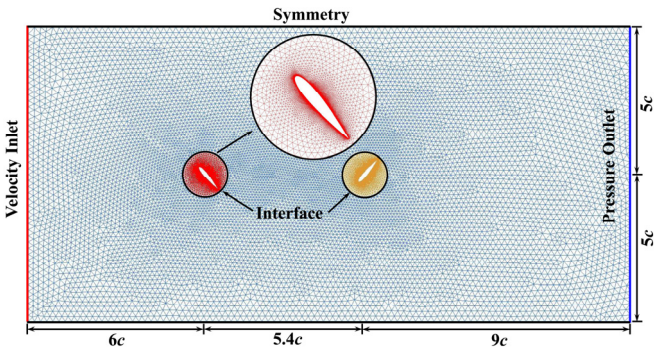

Fig. 2. Computational domain and mesh structures.

The sliding and dynamic mesh technologies are employed for the mesh treatment under the fluid-

structure interactions. Thus, the computational domain is divided into three parts. The two circular domains with a radius of 2.5c moves with the hydrofoil which is governed by the UDF and are connected to the outer domain through the non-conformal interfaces for an accurate flux exchange. The large deformation of outer domain meshes induced by the movement inner domains requires unstructured meshes. The structured meshes are used for the boundary layer around the foil surface. And y+ is controlled to below 1.

III. RESULTS AND DISCUSSION

The reduced frequency ($k = fc/U$) and pitching amplitude play an important role in the performance of energy harvesting of the tandem coupled flapping hydrofoils [16]. In this subsection, the effect of reduced frequency and pitching amplitude on the motion responses and power extraction is investigated.

The dimensionless cycle-averaged conversion efficiency η is defined for evaluating the hydrofoil performance of power extraction:

$$\eta = \frac{\int_t^{t+T} P\,dt}{\frac{1}{2}\rho U^3 dS} \tag{5}$$

where $P = T_L\omega + M\omega_p$, M is the pitching hydrodynamic torque act on the hydrofoil about the pitching axis, and ω_p is the pitching angular velocity. $M\omega_p$ is the pitching hydrodynamic power, and it is equal to the external power required to actuating the pitching motion in complete period without considering the mechanical and electric losses. d is the overall vertical extent of the hydrofoil motion. S is the span of the foil, and it is set as 1m in the reference value panel of Fluent.

The dimensionless cycle-averaged power coefficient C_P is defined as:

$$C_P = \frac{\int_t^{t+T} P\,dt}{\frac{1}{2}\rho U^3 cS} \tag{6}$$

The time histories of resultant torque coefficient C_T, heaving angular velocity ω and heaving $\alpha(t)$ is shown in Fig. 3. It can be seen that the variations of above three parameters all show the periodic characteristics after five periods. The peak values of C_T, ω and $\alpha(t)$ at stable stage are 12.5, 2.06 rad/s and 19.5°, respectively.

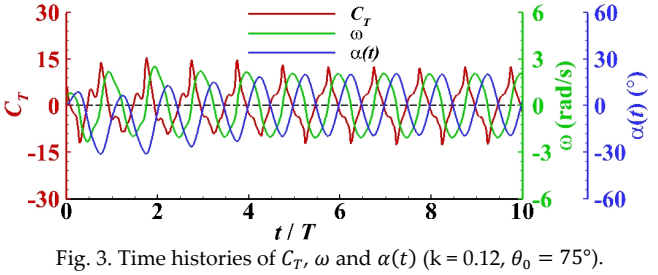

Fig. 3. Time histories of C_T, ω and $\alpha(t)$ (k = 0.12, θ_0 = 75°).

The power extraction efficiency and power coefficient variations with pitching amplitude at various reduced frequency are shown in Fig. 4. It can be seen that the efficiency increases first and then decrease with the increasing pitching amplitude. The peak values of 32.4%, 51.7% and 63.8% can be achieved at θ_0 = 75° for k = 0.06, 0.09 and 0.12, respectively. While the peak value of 52.8% for k = 0.15 is obtained at θ_0 = 60°, and the power efficiency decreases dramatically to 22.5% at θ_0 = 90°. And it should be noted that the motion for k = 0.15 and θ_0 = 90° would not enter a stable stage.

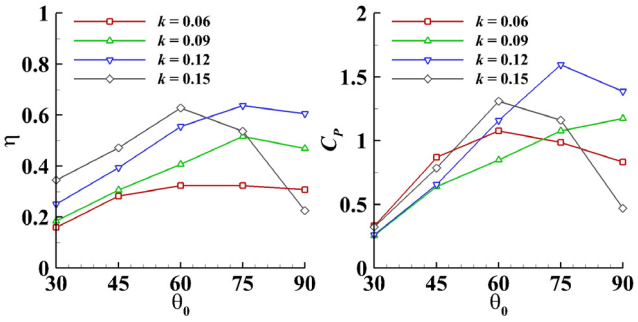

Fig. 4. η and C_P variations with θ_0 at various reduced frequency.

The trend of power coefficient variation is similar to the efficiency. As can been seen, C_P increases first and then decrease as pitching amplitude increases except the case of k = 0.09. The peak value is 1.59 for k = 0.12 at θ_0 = 75°.

The vorticity contours around the hydrofoil in a stable cycle for k = 0.06 and 0.12 are illustrated in Fig. 5. As can been seen, the reduced frequency has a significant effect on the timing of the generation, evolution, and shedding of vortices from the hydrofoil surface. Furthermore, due to the interaction between vortices of upstream hydrofoil and downstream hydrofoil, the effect of reduced frequency on the power extraction performance of the tandem hydrofoil configuration would be more significant than that of the single hydrofoil. At t = T / 4, significant LEV is observed at the middle chord of the foil and the trailing edge for both k = 0.06 and 0.12. In addition, a pair of vortexes shed off from the upstream foil and travel downstream for k = 0.06. At t = T / 2, vortexes which shed off from the surface of upstream hydrofoil has travelled downstream from the upward side of the downstream hydrofoil, and the interaction is relatively weak for k = 0.06. While the vortex in the case of k = 0.06 is just located at the middle of tandem hydrofoils. And this vortex collides with the downstream hydrofoil at t = 3T / 4 with a strong interaction.

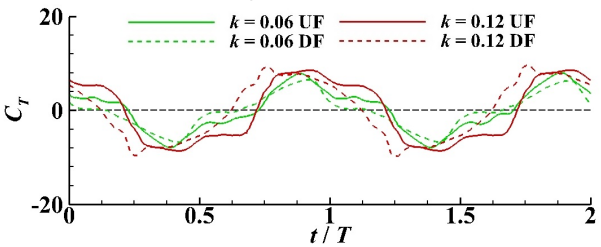

Fig. 6. Time histories of hydrodynamic torque coefficient.

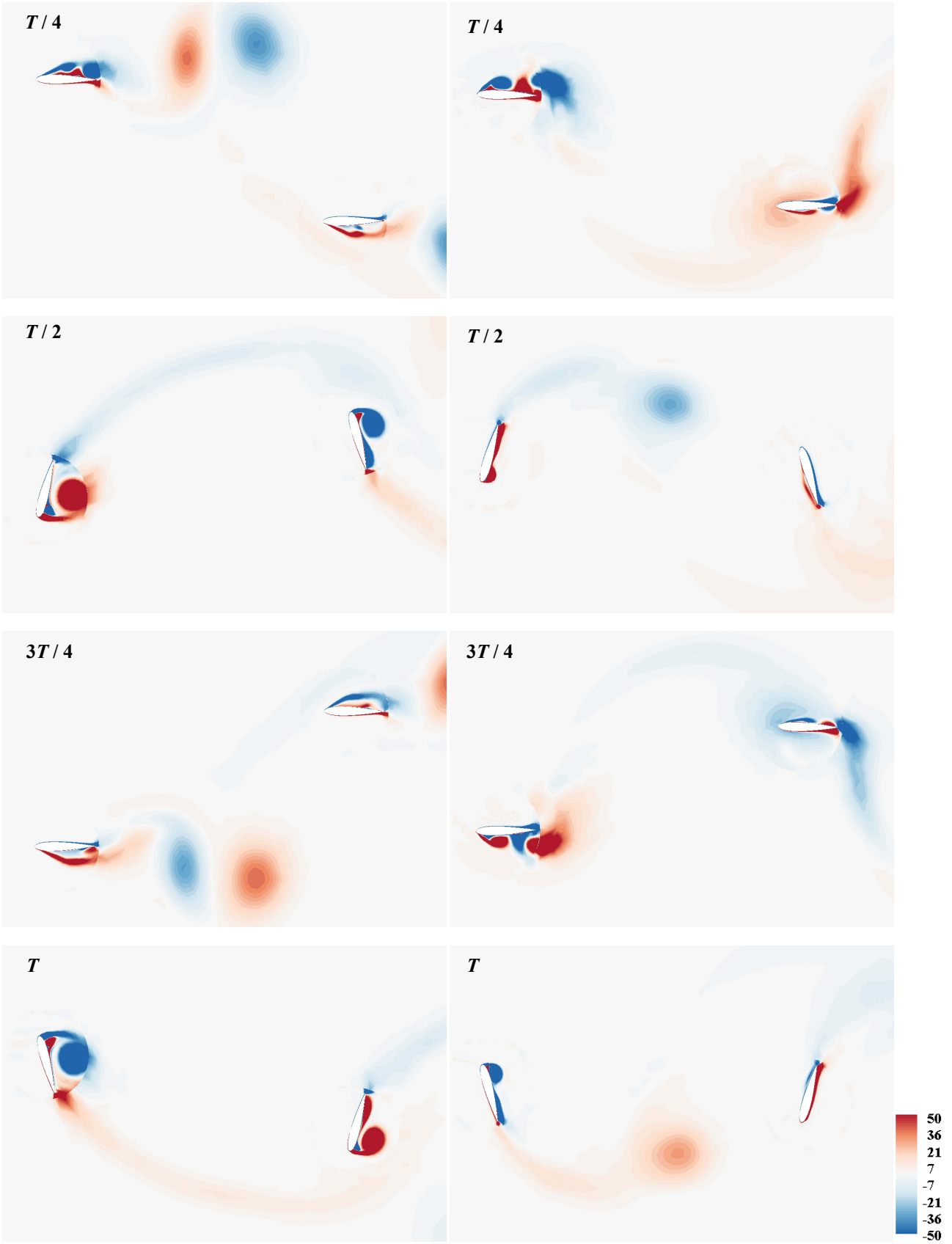

(a) k = 0.06 (b) k = 0.12

Fig. 5. Vorticity contours over the hydrofoil at different instants in a cycle.

The time histories of the hydrodynamic torque coefficient of upstream hydrofoil (UF) and downstream hydrofoil (DF) for k = 0.06 and 0.12 are shown in Fig. 6. It can be seen that the average value of positive torque coefficient of k = 0.12 ($\bar{C}_T$ = 5.97) is larger than that of k = 0.06 ($\bar{C}_T$ = 5.64), and the value of upstream hydrofoil ($\bar{C}_T$ = 3.87) is larger than that of downstream hydrofoil ($\bar{C}_T$ = 2.83). At t = T / 4 (3T / 4), the downstream hydrofoil is interacting with the vortex for k = 0.12. Thus, the torque coefficient of downstream hydrofoil is larger than that of

upstream hydrofoil. While the downstream hydrofoil is in weak interaction with vortex for $k = 0.06$, and the torque coefficients of upstream and downstream are similar.

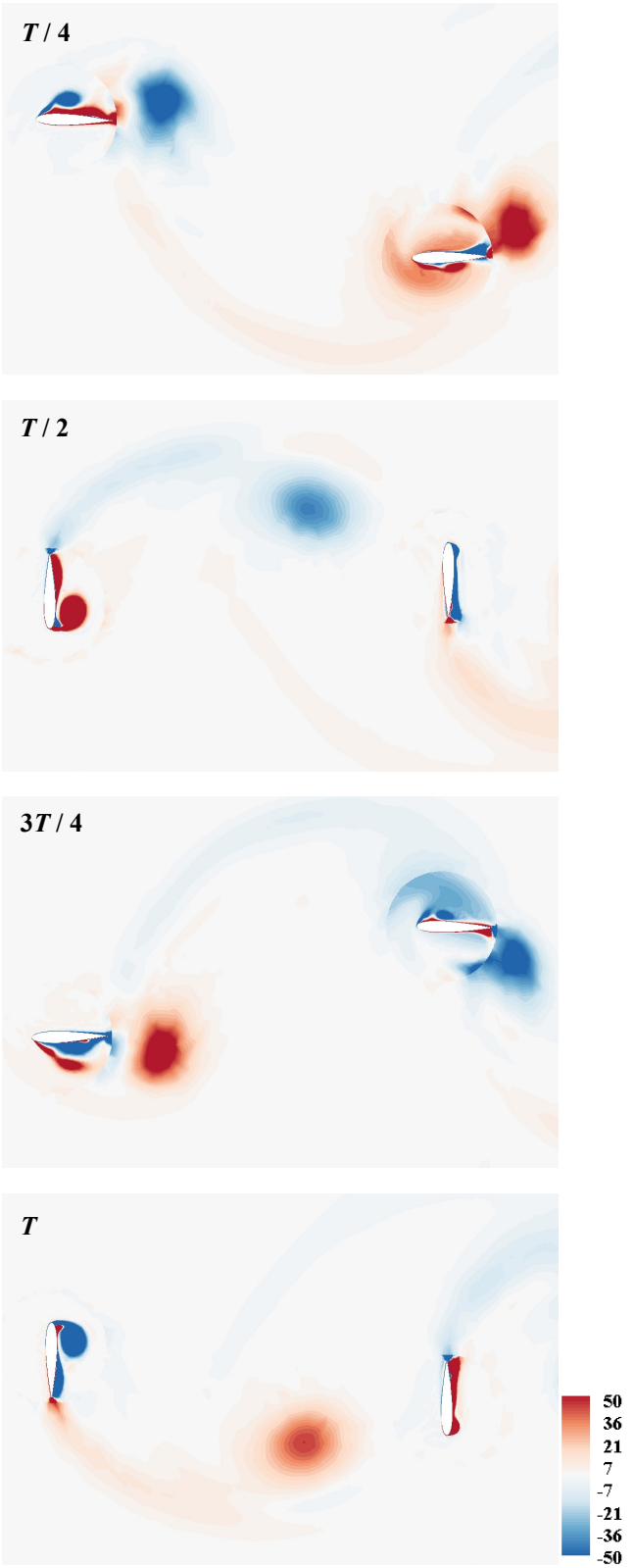

Fig. 7. Vorticity contours over the hydrofoil at different instants.

The vorticity contours around the hydrofoil in a stable cycle for $k = 0.12$ and $\theta_0 = 90°$ are illustrated in Fig. 7. The development trend of vortices is similar to that of $\theta_0 = 75°$, and the strength of vortices is more intense.

The time histories of the hydrodynamic torque coefficient of upstream hydrofoil (UF) and downstream hydrofoil (DF) for $\theta_0 = 75°$ and $90°$ are shown in Fig. 8. Mentioned as above, the vortex shed off from the upstream hydrofoil in the case of $\theta_0 = 90°$ is more intense than that of $\theta_0 = 75°$. The average value of positive torque coefficient of upstream hydrofoil is 37.7% higher than that of downstream hydrofoil for $\theta_0 = 90°$.

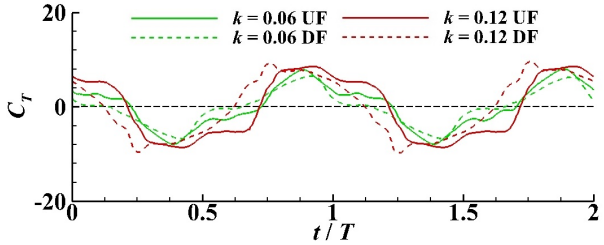

Fig. 8. Time histories of hydrodynamic torque coefficient.

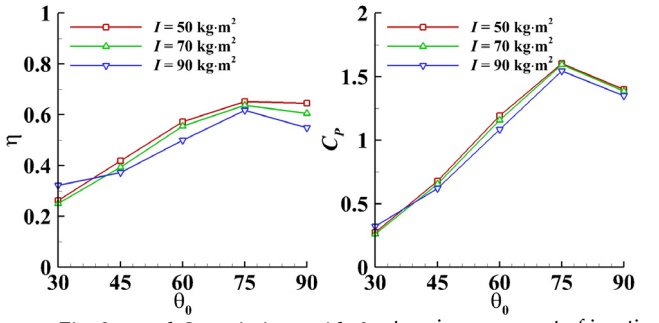

Fig. 9. η and C_P variations with θ_0 at various moment of inertia.

The power extraction efficiency and power coefficient variations with pitching amplitude at various moment of inertia are shown in Fig. 9. It can be seen that the moment of inertia affects the power extraction efficiency significantly, and the power coefficient is less affected by the moment of inertia. The efficiency decreases with the increasing moment of inertia except for $\theta_0 = 30°$. The peak value of efficiency is 65.2% obtained for $I = 50\text{kg·m}^2$ and $\theta_0 = 75°$.

IV. Conclusions and Future Works

A 2D fluid-structure interaction model is set up based on Fluent to investigate the power extraction performance of coupled tandem flapping hydrofoils. The effects of reduced frequency, pitching amplitude and moment of inertia on the power coefficient, efficiency and flow field are studied. The reduced frequency and pitching amplitude have a significant effect on the timing of the generation, evolution, and shedding of vortices from the hydrofoil surface. The interaction between the vortices and the downstream hydrofoil plays an important role on the performance of power extraction. The efficiency increases first and then decrease with the increasing pitching amplitude, and the peak value of power efficiency is found to be 63.8% for $\theta_0 = 75°$ and $k = 0.12$.

In the future work, more parameters will be employed to reveal the mechanism of fluid-structure interaction of tandem coupled hydrofoils, and the power extraction performance will be improved. A fully-passive pattern will be induced in the 2D numerical simulation. A 3D

numerical model will be established to understand the practical fluid-structure interaction of the coupled tandem hydrofoils.

REFERENCES

[1] Xiao Q, Zhu Q. A review on flow energy harvesters based on flapping foils[J]. Journal of fluids and structures, 2014, 46: 174-191.

[2] Xu J, Sun H, Tan S. Wake vortex interaction effects on energy extraction performance of tandem oscillating hydrofoils[J]. Journal of Mechanical Science and Technology, 2016, 30(9): 4227-4237.

[3] Young, John, Joseph CS Lai, and Max F. Platzer. "A review of progress and challenges in flapping foil power generation." Progress in aerospace sciences 67 (2014): 2-28.

[4] Kinsey, Thomas, and Guy Dumas. "Testing and analysis of an oscillating hydrofoils turbine concept." ASME Paper No. FEDSM-ICNMM2010-30869 (2010).

[5] Kinsey, T., et al. "Prototype testing of a hydrokinetic turbine based on oscillating hydrofoils." Renewable energy 36.6 (2011): 1710-1718.

[6] Kinsey, Thomas, and Guy Dumas. "Optimal tandem configuration for oscillating-foils hydrokinetic turbine." Journal of fluids engineering 134.3 (2012): 031103.

[7] Rival, David, Roland Manejev, and Cam Tropea. "Measurement of parallel blade–vortex interaction at low Reynolds numbers." Experiments in Fluids 49.1 (2010): 89-99.

[8] Zhu, Luoding. "Interaction of two tandem deformable bodies in a viscous incompressible flow." Journal of Fluid Mechanics635 (2009): 455-475.

[9] Karbasian, Hamid Reza, J. A. Esfahani, and E. Barati. "Simulation of power extraction from tidal currents by flapping foil hydrokinetic turbines in tandem formation." Renewable energy 81 (2015): 816-824.

[10] Jones, Kevin D., K. Lindsey, and M. F. Platzer. "An investigation of the fluid-structure interaction in an oscillating-wing micro-hydropower generator." WIT Transactions on The Built Environment 71 (2003).

[11] Broering, Timothy M., and Yongsheng Lian. "Numerical study of tandem flapping wing aerodynamics in both two and three dimensions." Computers & Fluids 115 (2015): 124-139.

[12] Xu, G. D., and W. H. Xu. "Energy extraction of two flapping foils with tandem configurations and vortex interactions." Engineering Analysis with Boundary Elements 82 (2017): 202-209.

[13] Xu, Jianan, Hongyu Sun, and Songlin Tan. "Wake vortex interaction effects on energy extraction performance of tandem oscillating hydrofoils." Journal of Mechanical Science and Technology 30.9 (2016): 4227-4237.

[14] Broering, Timothy M., and Yong-Sheng Lian. "The effect of phase angle and wing spacing on tandem flapping wings." Acta Mechanica Sinica 28.6 (2012): 1557-1571.

[15] Liu, Wendi. "A case study on tandem configured oscillating foils in shallow water." Ocean Engineering 144 (2017): 351-361.

[16] Sitorus, Patar Ebenezer, and Jin Hwan Ko. "Power extraction performance of three types of flapping hydrofoils at a Reynolds number of 1.7 E6." Renewable Energy 132 (2019): 106-118.